AIP | Applied Physics Letters

Theoretical study on the top- and enclosed-contacted single-layer MoS2 piezotronic transistors

Wei Liu, Yongli Zhou, Aihua Zhang, Yan Zhang, and Zhong Lin Wang

Citation: Applied Physics Letters **108**, 181603 (2016); doi: 10.1063/1.4948660
View online: http://dx.doi.org/10.1063/1.4948660
View Table of Contents: http://scitation.aip.org/content/aip/journal/apl/108/18?ver=pdfcov
Published by the AIP Publishing

Theoretical study on the top- and enclosed-contacted single-layer MoS_2 piezotronic transistors

Wei Liu,[1,a),b)] Yongli Zhou,[1,a)] Aihua Zhang,[1] Yan Zhang,[2] and Zhong Lin Wang[1,3,b)]
[1]*Beijing Institute of Nanoenergy and Nanosystems, Chinese Academy of Sciences, National Center for Nanoscience and Technology (NCNST), Beijing 100083, People's Republic of China*
[2]*Institute of Theoretical Physics, and Key Laboratory for Magnetism and Magnetic Materials of MOE, Lanzhou University, Lanzhou 730000, China*
[3]*School of Materials Science and Engineering, Georgia Institute of Technology, Atlanta, Georgia 30332, USA*

(Received 2 March 2016; accepted 25 April 2016; published online 4 May 2016)

Recently, the piezotronic effect has been observed in two-dimensional single-layer MoS_2 materials, which have potential applications in force and pressure triggered or controlled electronic devices, sensors, and human-machine interfaces. However, classical theory faces the difficulty in explaining the mechanism of the piezotronic effect for the top- and enclosed-contacted MoS_2 transistors, since the piezoelectric charges are assumed to exist only at the edge of the MoS_2 flake that is far from the electronic transport pathway. In the present study, we identify the piezoelectric charges at the MoS_2/metal-MoS_2 interface by employing both the density functional theory and finite element method simulations. This interface is on the transport pathway of both top- and enclosed-contacted MoS_2 transistors, thus it is capable of controlling their transport properties. This study deepens the understanding of piezotronic effect and provides guidance for the design of two-dimensional piezotronic devices. *Published by AIP Publishing.* [http://dx.doi.org/10.1063/1.4948660]

Piezotronic effect utilizes strain-induced piezoelectric charges (piezocharges) as a new means for "gating" the carrier transport,[1] which has been used to design and fabricate unique electromechanical functional devices such as nanogenerators,[2,3] logic devices,[4] flexible human-machine interfaces,[5] and photonic-strain sensor arrays.[6] Recently, piezoelectric and piezotronic effects have been observed in a single-atomic-layer MoS_2 for the first time,[7] broadening the field of piezotronics to the two-dimensional (2D) transition-metal dichalcogenide materials.[8] Our previous study has revealed the important role of the metal-MoS_2 interface in enhancing the piezotronic effect in an edge-contacted MoS_2 transistor by breaking the metallic states screening effect at the MoS_2 edge.[9] However, the previous theory did not give an apparent explanation of how the piezotronic effect arises in the top- and enclosed-contacted MoS_2 transistors, which are commonly fabricated in experiments.

Figure 1 shows the schematic illustration of the enclosed-contacted MoS_2 transistor. The polarization direction of the MoS_2 flake is pointed from the left-hand electrode to the right-hand electrode, paralleling to the transport direction. Since the thickness of the MoS_2 flake is of a single-atom dimension, the injected and outgoing charge carriers (electrons and holes) should follow the pathway at the MoS_2/metal-MoS_2 interface, which is marked in the figure by a black arrowhead; the part of the MoS_2 flake deep enclosed inside the electrode, on the other hand, is short-circuited. The transport pathway of the top-contacted transistor is similar to the pathway of the enclosed-contacted transistor (which is not shown in Fig. 1 to avoid the redundancy). According to the classical piezotronic theory, when an external strain is applied along the polarization direction, piezocharges are created at the two edges of the MoS_2 flake (refer to Fig. 1(a)), which is not on the transport pathway of the enclosed-contacted (top-contacted) transistor and thus should not control its transport characteristics. However, using the density functional theory (DFT) simulations in the present study, we show that the piezocharges indeed exist at the MoS_2/metal-MoS_2 interface (refer to Fig. 1(b)), which are on the transport pathway and are thus capable of controlling the transport properties of the transistor. The simulations focus on a structure consisting of two MoS_2/metal-MoS_2 interfaces and an inner MoS_2 region as enclosed

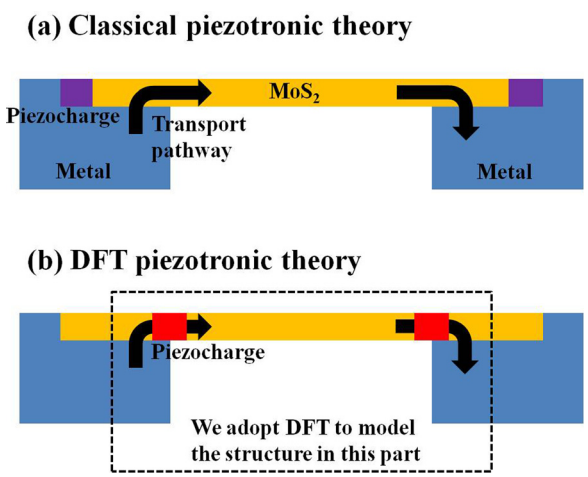

FIG. 1. Schematic illustration of the difference between the classical and DFT piezotronic theory on the piezocharge distribution in an enclosed-contacted MoS_2 transistor. (a) According to the classical theory, the piezocharges are distributed at the edges of the MoS_2 flake (purple), which is far from the electronic transport pathway (black arrow). (b) On the contrary, by the DFT theory, the piezocharges are predicted to exist at the MoS_2/metal-MoS_2 interfaces (red), which is on the transport pathway and thus is capable of controlling the transport characteristics.

[a)]W. Liu and Y. Zhou contributed equally to this work.
[b)]Authors to whom correspondence should be addressed. Electronic addresses: wliu@binn.cas.cn and zlwang@gatech.edu.

in the black dashed box in Fig. 1(b), which is a top-contacted configuration. Furthermore, we also adopt the finite-element method (FEM) to calculate the I-V curve of the transistors by including the piezocharge distribution as a parameter. The results of FEM calculations show that piezocharges distributed at the MoS_2/metal-MoS_2 interfaces (Fig. 1(b)) can effectively control the transport characteristics of the transistor while those at MoS_2 edges (Fig. 1(a)) cannot. The observation supports our DFT simulation results. This study not only furthers the understanding on the piezotronic effect but also provides guidance for the future design of 2D piezotronic devices.

First, the DFT study is adopted to calculate the piezocharge distribution at the MoS_2-MoS_2/Pd interface, which is the transition region between MoS_2 bare flake and MoS_2 top-contacted by Pd electrode. Figure 2(a) shows the atomic structure of the MoS_2 transistor. Pd is selected as the electrode metal.[7] In our simulation, a simple orthorhombic supercell is adopted, which is shown by a black box in Fig. 2(a). The size of the equilibrium cell is about 10 Å along x direction, 32 Å along y direction, and 34 Å along z direction. The Pd[111] direction is parallel to the z-axis and the MoS_2 layer is parallel to the xz plane. To eliminate the lattice mismatch between the Pd electrode and MoS_2 in the xz plane, the Pd electrode is stretched for 0.2% in both x and z directions, which does not give obvious influences on the electronic structure or Schottky barrier height at the metal-semiconductor interface.[10,11] Periodic boundary conditions are applied to all the x, y, and z directions of the supercell. The periodical boundary condition along the z direction results in the connection of the Pd electrodes in the neighboring supercells, which does not give obvious influence on the calculation results of the piezocharge distribution width and total amount of piezocharges. To avoid the interactions between neighboring supercell along the y direction, a vacuum layer with width of 16 Å is added to the supercell, which is sufficient in the convergence test. The external

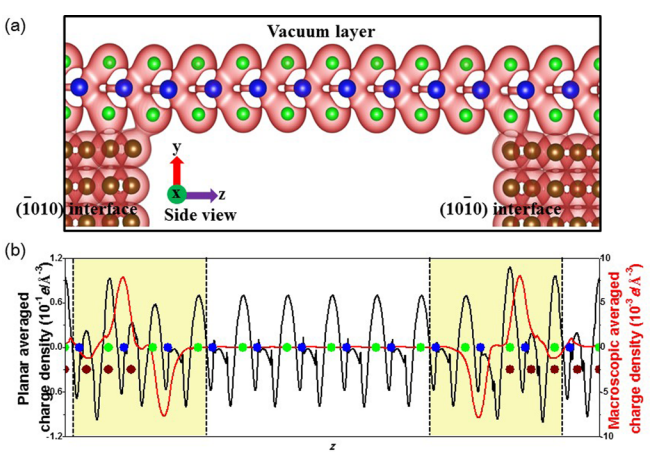

FIG. 2. (a) The atomic model of the MoS_2 transistor used in the DFT calculations. The isosurface of electron density with a level of 0.04 Å^{-3} is also shown in the figure. The black box denotes the boundary of the supercell in the yz plane. Note that only three layers of Pd atoms nearest to the MoS_2 flake along the y-axis are shown in the figure, other three layers are omitted to avoid redundancy. (b) The planar charge density (black line) and its double macroscopic average (red line) of the transistor long the z-axis. The piezocharge distribution region at each MoS_2-MoS_2/Pd interface is marked by a light yellow box. In the figures, the blue circles stand for Mo atoms, the green circles for S atoms, and the brown circles for Pd atoms.

strain, ranging from −5% to 5%,[12] is exerted on the transistor along the z-axis by compressing and/or stretching the cell constant of the equilibrium transistor while keeping the fractional coordinates of all atoms fixed. The structure optimization is performed on both equilibrium and strained transistors following the previously adopted method.[9] The Pd atoms in the two bottom layers along the y-axis are fixed in the optimization, since they are farthest to the MoS_2 flake and therefore hardly change positions in the optimization. Since there is no inversion symmetry in the transistor structure, the piezocharges will accumulate at two MoS_2-MoS_2/Pd interfaces under an external applied strain, leading to the piezotronic effect. Furthermore, as long as up to 5% strain is used in the present study, only minor relative movements happen on the Mo, S, and Pd atoms near the interface region, while other atoms in the inner MoS_2 and MoS_2/Pd regions do not change their fractional coordinates along the z axis. Thus, the strain field is almost uniform along the z direction of the supercell.

The DFT simulations of the MoS_2 transistors are performed by the Vienna *ab initio* simulation package (VASP)[13,14] with frozen-core projector-augmented-wave (PAW) pseudopotentials.[15,16] The exchange correlation potentials are treated by Perdew-Burke-Ernzerhof (PBE) parameterization within the general gradient approximation (GGA).[17] The *k*-point sampling mesh is $3 \times 1 \times 1$ in the structural optimization and $9 \times 1 \times 1$ in the properties calculations. Denser *k*-mesh in the structure optimization or property calculation does not provide obvious difference in the simulation results. A plane-wave energy cutoff of 400 eV is adopted in the simulations.[10]

The FEM simulations of the transistors based on COMSOL software have been done following the method employed in previous studies.[18] COMSOL software has been adopted in several FEM studies on the mechanical, piezoelectric, and transport properties of the atomic-thin 2D materials,[19,20] and the results of which agree well with the experiments.

Using the DFT calculations, we show here the piezocharge distribution at the MoS_2/Pd-MoS_2 interfaces of the transistors, which cannot be predicted by the classical piezotronic theory. The calculation of the piezocharge density follows our previously adopted method, which is based on the planar charge density.[9,12] First, the planar potential within the transistor supercell is obtained, which is a one-dimensional function depending only on the z-axis. Then by applying the Poisson's equation on the planar potential, the planar charge density can be obtained as shown in Fig. 2(b) by a black line. Periodical fluctuations of the planar charge density can be found in both deep MoS_2/Pd and MoS_2 regions as a result of the underlying atomic structures. These oscillations can be filtered out by a smoothing treatment called the double-macroscopic-average method,[21] from which the macroscopic charge density is obtained and shown by a red line in Fig. 2(b). The macroscopic charge density of the transistor becomes zero in both deep MoS_2/Pd and MoS_2 regions, indicating charge neutrality in these regions, which is consistent with the classical piezotronic theory. On the other hand, the macroscopic charge density shows an irregular shape in the transitional region sandwiched between the deep MoS_2/Pd and MoS_2, suggesting the formation of the

interface region. It is noteworthy that the Pd electrode plays an important role in forming the interface region in MoS_2 transistors. From the isosurface of the electron density shown in Fig. 2(a), the chemical bonding is formed between the MoS_2 and Pd, which modifies the electronic structure of the MoS_2 flake, thus resulting in the interface region between the MoS_2/Pd and MoS_2. Under an applied strain, the bound charges accumulate at two interface regions asymmetrically and become the piezoelectric charges, which increase the piezotronic effect.

According to the behavior of the macroscopic charge density, the transistor can be divided into several regions along the *z*-axis: the two regions where the macroscopic charge density varies obviously, as shown in Fig. 2(b) by light yellow, are picked as MoS_2/Pd-MoS_2 interface regions, while the two regions where the macroscopic charge density becomes almost zero, on the other hand, are picked as the deep MoS_2/Pd and deep MoS_2 regions. The piezocharges distribute at the interface region and the piezocharge density is obtained as the difference of the planar charge density between the transistor in equilibrium and the transistor under the strain. Figures 3(a) and 3(b) show the piezocharge density distributions at the $(\bar{1}010)$ and $(10\bar{1}0)$ interfaces, respectively, of the transistor under the applied strain $\pm 1\%$. Each piezocharge distribution region (interface region) includes three single columns of Mo-S atoms along the z-axis with a total width of 8.28 Å. Figures 3(c) and 3(d) show the total number of piezocharges divided by the transistor width (along x-axis) at the two interfaces, respectively. Under a compressive strain, the positive piezocharges accumulate at the $(\bar{1}010)$ interface and the negative piezocharges accumulate at the $(10\bar{1}0)$ interface, leading to the negative piezoelectric polarization along the z-axis. On the contrary, when a tensile strain is applied on the transistor, the negative piezocharges are at the $(\bar{1}010)$ interface and the positive piezocharges are at the $(10\bar{1}0)$ interface, which is opposite to the case under the compressive strain, thus resulting in the positive piezoelectric polarization. This observation is consistent with the classical piezotronic theory. For comparison, we also calculate the total number of charges of a single-column MoS_2 in the deep MoS_2/Pd or MoS_2 region, which is always zero and does not vary under different strains, indicating that the piezocharges distribute only at the interface region. It is worth noting that the piezocharges of the top- and enclosed-contacted transistors originate from the single-layer atomic structure of the MoS_2 flake, the electronic structure of which can be modified by the Pd electrode, thus forming the MoS_2/Pd-MoS_2 interface region where the piezocharges accumulate under the applied strain. Due to the above reason, the prediction of the piezocharge distribution must resort to the DFT based quantum mechanical simulation.

Next, we perform the FEM simulations on the I-V curve and charge carrier concentrations of the top- and enclosed-contacted MoS_2 transistors under the external applied strains, adopting the DFT obtained piezocharge distribution width as a parameter. The FEM simulations use the method similar to the previous study.[18] The single-layer MoS_2 flake used in the present study has a length of 100 nm along the transport direction, with a 10 nm part at each end top-contacting/enclosed-contacting by the Pd electrode (refer to Fig. 4). The width of the flake is 10 nm, while the thickness is 0.65 nm. In order to examine the piezotronic effect of the piezocharges at different places, we construct the "edge" (Fig. 4(a)) and "interface" (Fig. 4(b)) models, in which the piezocharges distribute at the MoS_2 edges and MoS_2/Pd-MoS_2 interfaces, respectively. The width of the piezocharge distribution region is 8.28 Å, which is obtained from the DFT calculation. Here, we would like to emphasize that, although the MoS_2 flake used in the FEM simulation is much longer than the model in DFT study along the transport direction, the transport characteristic of the 100 nm-long MoS_2 flake under the piezotronic effect is mainly influenced by the piezocharges at the transistor interfaces, which is distributed in the region shorter than 1 nm and thus can be obtained by DFT simulations.

Using the enclosed-contacted transistor as an example, Fig. 4(a) shows the I-V curve of the edge model, which does

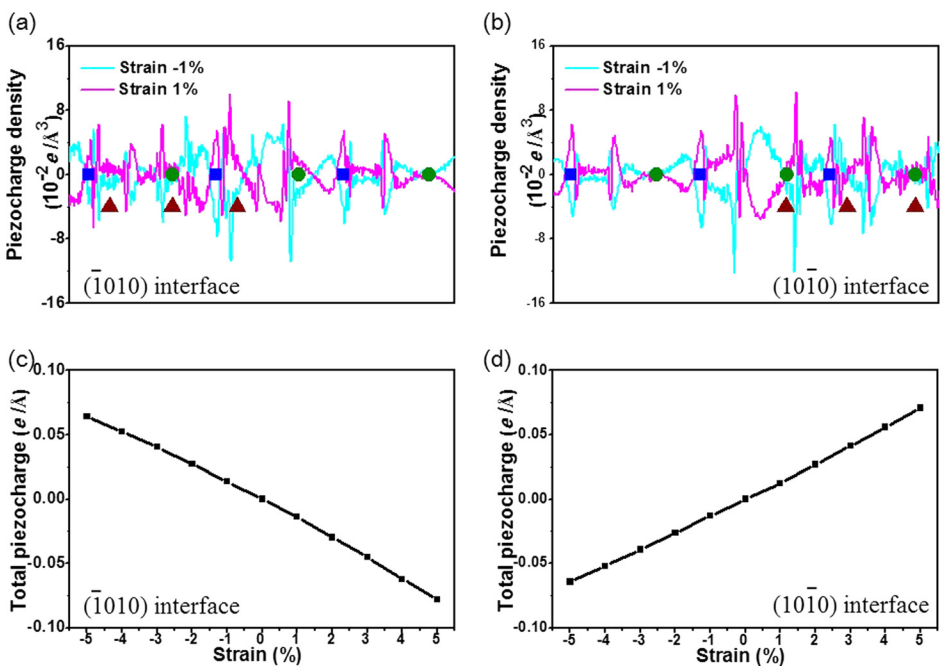

FIG. 3. Piezocharge distributions and total number of piezocharges at interfaces obtained by the DFT simulations. (a) and (b) The piezocharge distributions of the transistor at the $(\bar{1}010)$ and $(10\bar{1}0)$ interfaces, respectively. In the two figures, the blue squares stand for the positions of Mo atoms, the green circles for the positions of S atoms, and the brown triangles for the positions of Pd atoms. (c) and (d) The total number of piezocharges per transistor width at the $(\bar{1}010)$ and $(10\bar{1}0)$ interfaces, respectively.

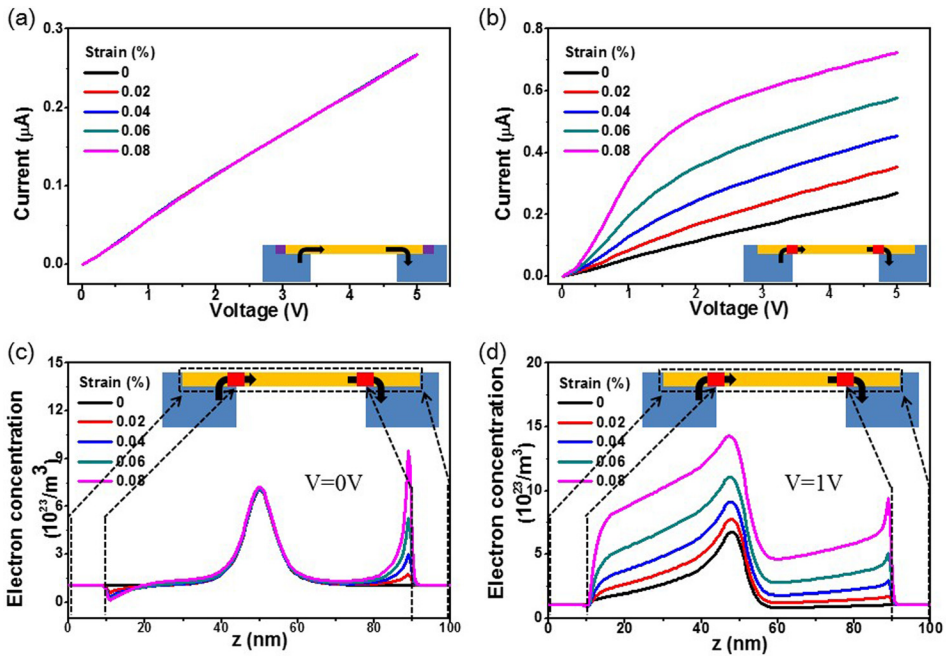

FIG. 4. Transport characteristics of the enclosed-contacted transistors obtained by the FEM simulations. (a) and (b) The I-V curves of the enclosed-contacted transistor under the external applied tensile strains, with the piezocharges at the MoS_2 flake edges and MoS_2/Pd-MoS_2 interfaces, respectively. (c) and (d) The electron concentrations in the MoS_2 flake along the transport direction in the case that the bias voltages are 0 and 1 V, respectively, with the piezocharges at the MoS_2/Pd-MoS_2 interfaces.

not show obvious dependence on the external applied strain. As mentioned earlier in this article, the classical piezotronic theory assumes that piezocharges distribute at the two edges of the MoS_2 flake, which, according to the results in Fig. 4(a), is invalid in explaining the piezotronic effect in the single-layer top- and enclosed-contacted MoS_2 transistors. On the other hand, by using the DFT simulation in the present study, we propose the interface model of the piezocharge distribution, in which the transport pathway goes through the MoS_2/Pd-MoS_2 interface region, thus the charge transport characteristics can be controlled by the applied strain as shown in Fig. 4(b). Figures 4(c) and 4(d) show the electron concentrations in the flake along the transport direction with the left-hand electrode under biases of 0 V and 1 V, respectively, of the interface model of the enclosed-contacted transistor. Under the tensile strain, negative piezocharges are created at the left-hand side interface [$(\bar{1}010)$ interface], repelling electrons, and thus forming the valley at the interface (near $z = 10$ nm in Figs. 4(c) and 4(d)); at the same time, the positive piezocharges are created at the right-hand side interface [$(10\bar{1}0)$ interface], attracting the electrons and therefore forming the peak at the interface (near $z = 90$ nm). Negative piezocharges raise the local Schottky barrier at the $(\bar{1}010)$ interface, while positive piezocharges lower the barrier at the $(10\bar{1}0)$ interface. For a positive bias applied on the left-hand electrode, the dominant barrier that dictates the I-V curve is the reversely biased interface at the right-hand side, at which the local barrier height is lowered by the piezocharges, resulting in an increase in the charge current under the tensile strain as shown in Fig. 4(b). Furthermore, for the part of the MoS_2 flake at each end that enclosed by the Pd electrode (z is from 0 to near 10 nm at the left-hand side or from near 90 to 100 nm at the right-hand side), its electron concentration keeps constant along the z-axis and hardly affected by both the bias voltage and applied strain, indicating the part of the flake is under the short-circuited condition. For further investigation, we also simulate the I-V curve and electron concentration of the top-contacted transistor; the results are similar to the enclosed-contacted transistors, indicating the top- and enclosed-contacted transistors have the same transport pathway across the MoS_2/Pd-MoS_2 interface thus the same mechanism of the piezotronic effect. The COMSOL simulation in the current section has verified our assumption earlier and the DFT results on the piezocharge distribution, which explained the experimental findings.

In summary, in the present study, we have theoretically examined the piezocharge distributions in the top- and enclosed-contacted single-layer MoS_2 transistors and their influences on the transport characteristics. First, by using the DFT simulation, we find piezocharges exist at the MoS_2/Pd-MoS_2 interface and obtain the piezocharge distribution width. This finding is beyond the scope of the classical piezotronic theory. Next, taking the piezocharge distribution width obtained above as a parameter, we perform the FEM simulation to obtain the I-V curve and electron concentration of the transistors under applied strains, which verified DFT results on distribution of the piezocharges at the MoS_2/Pd-MoS_2 interface. This study deepens the understanding of the piezotronic theory on the 2D material devices and will serve for the future design and optimization of piezotronic devices.

This work was supported by the "Thousands Talents" Program for Pioneer Researcher and His Innovation Team, China, and the National Natural Science Foundation of China (Grant No. 51432005).

[1]Z. L. Wang, *Piezotronics and Piezo-Phototronics* (Springer, Berlin, Heidelberg, 2013).
[2]Z. L. Wang and X. Wang, Nano Energy **14**, 1 (2015).
[3]Y. Zhang, C. Liu, J. Liu, J. Xiong, J. Liu, K. Zhang, Y. Liu, M. Peng, A. Yu, A. Zhang, Y. Zhang, Z. Wang, J. Zhai, and Z. L. Wang, ACS Appl. Mater. Interfaces **8**, 1381 (2016).
[4]R. Yu, W. Wu, C. Pan, Z. Wang, Y. Ding, and Z. L. Wang, Adv. Mater. **27**, 940 (2015).
[5]W. Wu, X. Wen, and Z. L. Wang, Science **340**, 952 (2013).
[6]C. Pan, L. Dong, G. Zhu, S. Niu, R. Yu, Q. Yang, Y. Liu, and Z. L. Wang, Nat. Photonics **7**, 752 (2013).

[7]W. Wu, L. Wang, Y. Li, F. Zhang, L. Lin, S. Niu, D. Chenet, X. Zhang, Y. Hao, T. F. Heinz, J. Hone, and Z. L. Wang, Nature **514**, 470 (2014).
[8]L. Chen, F. Xue, X. Li, X. Huang, L. Wang, J. Kou, and Z. L. Wang, ACS Nano **10**, 1546 (2016).
[9]W. Liu, A. Zhang, Y. Zhang, and Z. L. Wang, Appl. Phys. Lett. **107**, 083105 (2015).
[10]C. Gong, L. Colombo, R. M. Wallace, and K. Cho, Nano Lett. **14**, 1714 (2014).
[11]Y. Dong and L. J. Brillson, J. Electron. Mater. **37**, 743 (2008).
[12]W. Liu, A. Zhang, Y. Zhang, and Z. L. Wang, Nano Energy **14**, 355 (2015).
[13]G. Kresse and J. Hafner, Phys. Rev. B **48**, 13115 (1993).
[14]G. Kresse and J. Furthmüller, Phys. Rev. B **54**, 11169 (1996).
[15]P. E. Blöchl, Phys. Rev. B **50**, 17953 (1994).
[16]G. Kresse and D. Joubert, Phys. Rev. B **59**, 1758 (1999).
[17]J. P. Perdew, K. Burke, and M. Ernzerhof, Phys. Rev. Lett. **77**, 3865 (1996).
[18]Y. Zhang, Y. Liu, and Z. L. Wang, Adv. Mater. **23**, 3004 (2011).
[19]P. Butti, I. Shorubalko, U. Sennhauser, and K. Ensslin, J. Appl. Phys. **114**, 033710 (2013).
[20]M. Zelisko, Y. Hanlumyuang, S. Yang, Y. Liu, C. Lei, J. Li, P. M. Ajayan, and P. Sharma, Nat. Commun. **5**, 4284 (2014).
[21]J. Junquera, M. H. Cohen, and K. M. Rabe, J. Phys.: Condens. Matter **19**, 213203 (2007).